Hindawi Publishing Corporation
Advances in Materials Science and Engineering
Volume 2016, Article ID 5380835, 10 pages
http://dx.doi.org/10.1155/2016/5380835

Research Article

Influence of Concrete Properties on Molten Core-Concrete Interaction: A Simulation Study

Jin-yang Jiang,[1] Ying-jun Yu,[1,2] Hong-yan Chu,[1] Wei Sun,[1] and Yun Gao[1]

[1]*School of Materials Science and Engineering, Southeast University, Nanjing 211189, China*
[2]*Central Research Institute of Building and Construction Co., Ltd., Beijing, China*

Correspondence should be addressed to Jin-yang Jiang; jiangjinyang16@163.com

Received 20 May 2016; Revised 14 October 2016; Accepted 23 October 2016

Academic Editor: Patrice Berthod

In a severe nuclear power plant accident, the molten core can be released into the reactor pit and interact with sacrificial concrete. In this paper, a simulation study is presented that aims to address the influence of sacrificial concrete properties on molten core-concrete interaction (MCCI). In particular, based on the MELCOR Code, the ferrosiliceous concrete used in European Pressurized Water Reactor (EPR) is taken into account with respect to the different ablation enthalpy and Fe_2O_3 and H_2O contents. Results indicate that the concrete ablation rate as well as the hydrogen generation rate depends much on the concrete ablation enthalpy and Fe_2O_3 and H_2O contents. In practice, the ablation enthalpy of sacrificial concrete is the higher the better, while the Fe_2O_3 and H_2O content of sacrificial concrete is the lower the better.

1. Introduction

In a simulated core melt accident of nuclear power plant (NPP), a molten pool called corium can melt through the reactor pressure vessel (RPV) and be released to the containment basemat. Driven by the decay power of the fission products and the high temperature, the basemat concrete, which is the last barrier that prevents leakage of the radioactive products into environment in the second-generation NPPs, starts to ablate [1, 2]. Thus, the molten core-concrete interaction (MCCI) is of great importance in NPP because it may result in leakage of fission products. Previous studies show that the concrete properties have significant impact on MCCI [1–6]. In the third-generation NPPs, such as European Pressurized Water Reactor (EPR) [7], a core catcher is introduced to encase the corium, through which the integrity of the containment is preserved. Moreover, a specific ferrosiliceous sacrificial concrete containing both siliceous and hematite aggregates is employed in the reactor pit of EPR. The role of the sacrificial concrete is to adjust the properties of the corium released from RPV in terms of the interaction between them (MCCI). An investigation carried out by Chu et al. [8] has recently presented a systematic study on thermal properties of ferrosiliceous sacrificial concrete subjected to high temperatures, and another report focusing on the mechanical and physicochemical properties of ferrosiliceous concrete at high temperatures has also been recently published [9]. However, the ablation behavior or MCCI of ferrosiliceous concrete has not been studied in these literatures.

Wang et al. [10] have conducted a simulation investigation on core thermal response during a station blackout initiated severe accident in China pressurized reactor (CPR1000) using MELCOR Code, and the safety of the reactor core has been assessed. Nie [11] has made a systematic research on temporary melt retention in the reactor pit of EPR and has pointed out that, for a large breach loss of coolant accident scenario in the EPR, 1.20×10^5 kg of metallic melt and 1.85×10^5 kg of oxidic melt are released in the reactor pit, and the decay heat decreases from 32 MW (3 h after scram) to 20 MW (30 h after scram). Nevertheless, the concrete used in the CPR1000 was not the ferrosiliceous sacrificial concrete. Due to the complexity of MCCI, information on this phenomenon is still limited and needs to be updated.

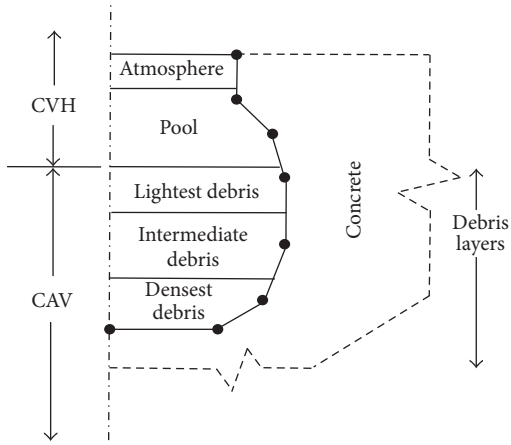

Figure 1: The cavity contents and boundary conditions [12].

This paper focuses on the influence of ferrosiliceous concrete properties on the MCCI, including the concrete ablation enthalpy and the Fe_2O_3 and H_2O contents. In the work, a simulation study is performed based on the MELCOR Code used for CPR1000. The calculation model is established by replacing the concrete cavity of a 1000 MW pressurized reactor (CPR1000) by the EPR reactor pit which employed the special ferrosiliceous sacrificial concrete. In essence, it is assumed that the interaction is induced by a typical small break loss of coolant severe accident sequence (SBLOCA) of the CPR1000, but the concrete cavity in the current study has been replaced by the ferrosiliceous sacrificial concrete cavity.

2. Main Assumptions for the Calculation

MELCOR is a fully integrated, engineering-level computer code that consists of various modules and packages [12]. The MELCOR Cavity (CAV) package models the attack of hot (often molten) core materials on the basemat concrete [14], and the cavity contents and boundary conditions are shown in Figure 1.

In the CAV package, two modes can be selected for the configuration of the core melt, that is, enforced mixing or enforced stratification. The enforced mixing is the simplest mode which considers the melt being a single layer. For the enforced stratification mode, the configuration of the melt is determined by the specific density of each layer. The most common structure is a three-layer configuration, where a metallic layer (MET) exists between the light oxide layer (LOX) and the heavy oxide layer (HOX). Another factor influencing the configuration of core melt is the rising gas bubbles generated by concrete decomposition, which promotes the mixing of different layers. In Sections 3.1 and 3.2, the configurations of core melt are assumed to be enforced mixing. In Section 3.3, with respect to the impact of rising gas bubbles, the configuration of core melt is assumed to be enforced stratification that shall address the influence of H_2O content. The ablation behavior of sacrificial concrete depends on the heat transferred from melt to it. The heat in the cavity comes from two sources, that is, the decay power from fission products (FP) and the chemical reaction taking place in the melt. The heat is transferred either through the top surface of the debris or to the concrete basemat and sidewalls, as determined by the thermal resistances.

In regard to the thermal resistance at MCCI, there are also two models to be selected, that is, the gas film model and the slag film model. For the gas film model, the dominant heat transfer mode is bubble-enhanced heat transfer determined by Greene correlation [15]. For the slag film model, intermittent melt-concrete contact results in periodic growth and removal of slag from the interface, and thus a modified version of the Kutateladze correlation [16] is used for bubbling heat transfer coefficient. In addition, a solid crust may be formed at the interface between sacrificial concrete and melt with heat transfer by thermal conduction. The solid crust hinders the contact of melt with concrete and decreases the heat transfer from melt to sacrificial concrete. In the paper, the slag film model is selected for both bottom and radial thermal resistance, because, under the postulated severe accident, superficial gas velocity is much lower and cannot form a stable gas film [17].

Another important parameter that affects sacrificial concrete ablation is the temperature at MCCI, which is defined as the ablation temperature of sacrificial concrete in MELCOR. The ablation temperature of ferrosiliceous sacrificial concrete used in the study is 1453 K, according to [1].

A typical small break loss of coolant severe accident sequence (SBLOCA) of the 1000 MW EPR NPP is assumed in this study. Before the accident, the EPR operates at full power with the thermal power of 3426 MW and the average coolant temperature of 566 K. Time zero in the calculation corresponds to the time of the reactor scram. Upon a stable calculation, that is, −550~0 s, the break initiates. No safety intervention is applied during the accident process. At 4360 s, the RPV was melted through. After that, the corium was poured into the sacrificial concrete pit mainly at two periods, 4360~5000 s and 7455~9767 s, and the mass of the corium in these two periods is 0.72×10^5 and 0.54×10^5 kg, respectively. The total mass of corium released to the reactor pit is about 1.26×10^5 kg.

The MELCOR decay heat package models the decay heat power resulting from the radioactive decay of fission products. In the study, the whole decay heat power was set according the CPR1000. The evolution of decay heat, heat loss to sacrificial concrete, and heat loss from debris surface is shown in Figure 2. And the decay heat, heat loss to sacrificial concrete, and heat loss from debris surface are not changed after 14500 s.

The material in reactor pit is made up of the ferrosiliceous sacrificial concrete with high content of Fe_2O_3. The composition and properties of sacrificial concrete input for calculation are shown in Tables 1 and 2, respectively. The geometry of the initial concrete cavity is cylindrical with a height of 4.95 m, radius of 3.075 m, basemat axial thickness of 0.45 m, and radial thicknesses of 0.55 m. The calculations are processed until axial melt-through. In addition, the maximum radius ablation depth is around 0.31 m.

In the paper, we supposed that the ablation behavior of sacrificial concrete was isotropic. An investigation by Sevón

Table 1: The composition of ferrosiliceous concrete [1].

Composition	SiO_2	Fe_2O_3	CaO	MgO	Al_2O_3	CO_2	H_2O_{EVAP}	H_2O_{CHEM}
Wt. (%)	44.4	32.3	12.4	1.0	3.2	2.3	2.4	2.0

Table 2: The properties of ferrosiliceous concrete [1].

Properties	Density/(kg/m^3)	Solidus temperature/K	Liquidus temperature/K	Ablation temperature/K
Values	2620	1433	1703	1453

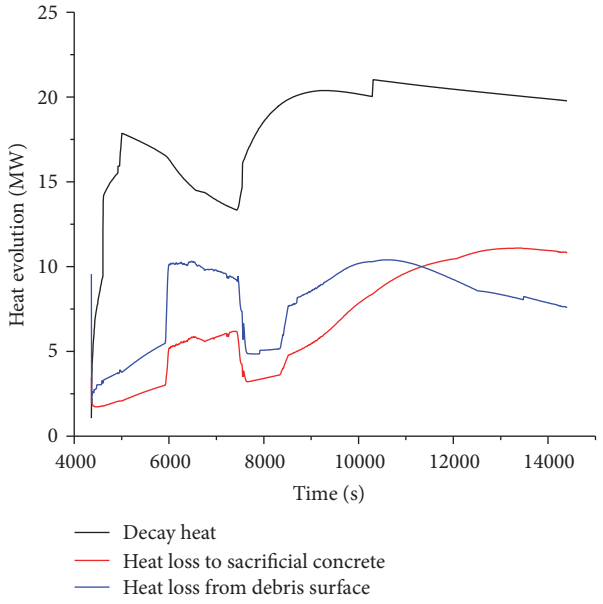

Figure 2: The evolution of decay heat, heat loss to sacrificial concrete, and heat loss from debris surface in the calculation.

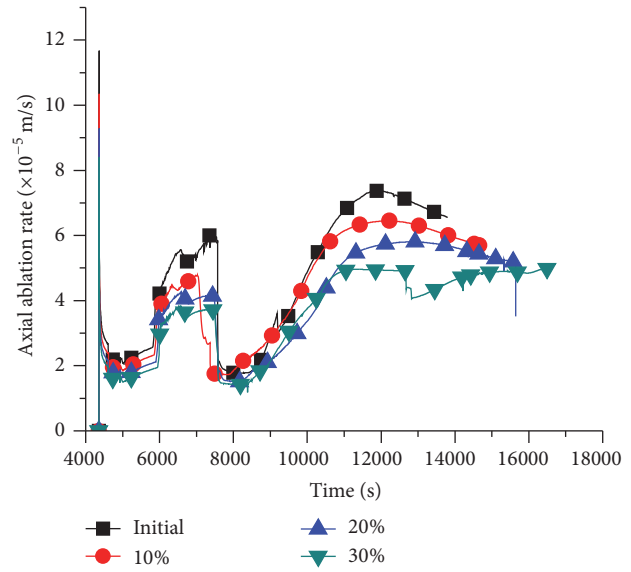

Figure 3: Sacrificial concrete ablation rate under different ablation enthalpy.

et al. [2] has shown that an anisotropic ablation pattern is observed for ferrosiliceous sacrificial concrete, but this result is based on small scale of MCCI. On the whole, however, the isotropic assumption was reasonably taken to evaluate the MCCI as it maximizes basemat ablation.

3. Results and Discussion

3.1. Ablation Enthalpy. Sacrificial concrete ablation enthalpy quantifies the heat required to convert a unit mass of virgin sacrificial concrete into condensed and gaseous decomposition products at the specified ablation temperature. Ablation enthalpy not only modifies the sacrificial concrete ablation heat but also changes the energy balance of ablation. For ferrosiliceous sacrificial concrete, the value of 1730 kJ/kg could be assigned as its ablation enthalpy, according to literature [18]. In this study, an increased ablation enthalpy of 10%, 20%, and 30% shall be performed to address its effect on the MCCI behavior.

As shown in Figure 3, the sacrificial concrete ablation rate shows a "peak-valley" tendency which may result from a "form-melt-reform-remelt" process of the crust. As the sacrificial concrete ablation enthalpy increases, the ablation rate decreases. In consequence, the melt-through time increases. At the elapsed time of 4360~5800 s and 7300~8700 s, the low and stable ablation rate of 2.2×10^{-5} m/s can be detected, which is attributed to the crust formed at the interface. Thereafter, the ablation rate increases rapidly. The maximum ablation rate of the initial (control) sacrificial concrete is 7.0×10^{-5} m/s. When the ablation enthalpy increases by 30%, the value of that is 4.7×10^{-5} m/s. Besides that, the melt-through time of the initial sacrificial concrete is 9442 s. When the ablation enthalpy increases by 10%, 20%, and 30%, the melt-through time is 10332 s, 11283 s, and 12245 s, respectively. As the melt is released from RPV to the pit, the melt temperature displays a rapid increase, as shown in Figure 4, the result of which is due to the decay heat released by fission products. The temperature decreases gradually after 5800 s upon the mixing of cold sacrificial concrete decomposition products with the melt. Similar to the sacrificial concrete ablation rate, the hydrogen generation rate also shows a "peak-valley" tendency, as illustrated in Figure 5. Minor discrepancies can be detected for the sacrificial concretes with varying ablation enthalpy. It might be due to the longer melt-through time for sacrificial concrete with larger ablation enthalpy. Thus, if the ablation enthalpy of sacrificial concrete is increased through mix design, then the melt-through time is prolonged, which is paramount for nuclear accident mitigation.

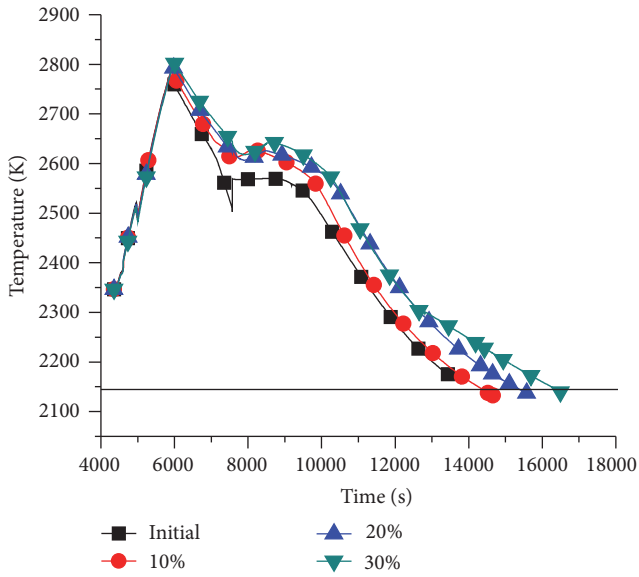

Figure 4: Temperature under different ablation enthalpy.

Past studies have suggested that concrete ablation in essence depends on the heat transfer from the melt pool to concrete. In this way, the concrete ablation rate can be expressed as follows [13]:

$$v = \frac{\dot{Q}}{\rho A \Delta H}, \tag{1}$$

where $\dot{Q}$ is the heat flux to concrete, ρ is the concrete density, ΔH is the concrete decomposition enthalpy, and A is the area of the ablating concrete. In practice, the heat conducted into concrete can be ignored with respect to the low thermal conductivity of concrete. Equation (1) suggests that when the concrete decomposition enthalpy increases, the concrete ablation rate decreases. In other words, upon the same heat flux, the concrete will be ablated more for the concrete with smaller decomposition enthalpy. Thus, as the mixed cold concrete decomposition products increase, the melt temperature decreases faster. Meanwhile, since H_2O is produced from the concrete decomposition, the hydrogen generation rate is closely related. As shown in Figure 5(b), the tendency of hydrogen generation rate is similar to the sacrificial concrete ablation rate.

3.2. Fe_2O_3 Content. As aforementioned, the sacrificial concrete is critical to the core catcher in EPR pit. It mainly contains Fe_2O_3 and SiO_2 with the total content reaching 76.7% [1, 2]. Previous studies indicated that heat released from the interactions of Fe_2O_3 and SiO_2 with zirconium accounts for the ablation of concrete [17]. For the sake of illustration, the reaction equations are presented, that is, (2)–(4). It can be noted that the heat with the Fe_2O_3—Zr reaction varies from that with the SiO_2—Zr reaction, especially at the temperature above 2143 K. Thus, the Fe_2O_3 content shall be of paramount importance for the MCCI. The Fe_2O_3 content in ferrosiliceous sacrificial concrete is around 32~36% [1]. In the KAPOOL tests, this value was chosen at 48% [3]. In this paper, the Fe_2O_3 content is chosen at 32.3%, 36%, and 48%. Meanwhile, the SiO_2 content is adjusted to ensure the sum of Fe_2O_3 and SiO_2 at 76.7%.

$$\mathrm{Zr} + \mathrm{SiO_2} \longrightarrow \mathrm{ZrO_2} + \mathrm{Si} + 1.6\,\mathrm{MJ/kg\ Zr} \quad (T < 2143\,\mathrm{K}) \tag{2}$$

$$\mathrm{Zr} + 2\mathrm{SiO_2} + 4.7\,\mathrm{MJ/kg\ Zr} \longrightarrow \mathrm{ZrO_2} + 2\mathrm{SiO\,(g)} \quad (T > 2143\,\mathrm{K}) \tag{3}$$

$$3\mathrm{Zr} + 2\mathrm{Fe_2O_3} \longrightarrow 3\mathrm{ZrO_2} + 4\mathrm{Fe} + 5.8\,\mathrm{MJ/kg\ Zr} \tag{4}$$

As shown in Figures 6–8, with the increased Fe_2O_3 content, both the sacrificial concrete ablation rate and the hydrogen generation rate increase, while the melt temperature decreases faster. In particular, the maximum sacrificial concrete ablation rate for the 48% Fe_2O_3 content is about 1.4 times that for the 32.3% Fe_2O_3 content. The melt-through time of sacrificial concrete decreases from 9442 s to 9131 s to 8193 s. In addition, the maximum temperature difference reaches 223 K, as compared to the concretes of 32.3% and 48% Fe_2O_3 contents. The mass of generated hydrogen is 102.6 kg for the sacrificial concrete with 32.3% Fe_2O_3 content. However, sacrificial concrete with 48% Fe_2O_3 content generates slightly less hydrogen, that is, 96.9 kg, the result of which is in line with literature [3].

Figure 9 indicates that the heat loss to sacrificial concrete increases with the increase of Fe_2O_3 content. Also, it reveals the reason why the sacrificial concrete ablation rate increases with the increase of Fe_2O_3 content. Above 2143 K, the SiO_2—Zr reaction is endothermic and the Fe_2O_3—Zr reaction is exothermic. Below 2143 K, the heat released from the Fe_2O_3—Zr reaction is higher than the SiO_2—Zr reaction upon the oxidation of same amount of Zr. It should be noted that, in the calculation except the very last instants of MCCI, SiO_2—Zr interaction is endothermal in the bulk of the pool, as shown in Figures 4 and 7 (the horizontal full line at 2143 K). Thus, the higher Fe_2O_3 content leads to the higher heat loss to sacrificial concrete. Figure 10 presents that the enthalpy of SiO_2 is higher than that of Fe_2O_3. At the ablation temperature of 1453 K, the ablation enthalpy shall be lower for the sacrificial concrete with higher Fe_2O_3 content. It is another reason for the faster ablation of the sacrificial concrete with higher Fe_2O_3 content. Therefore, the melt-through time can be extended by decreasing the Fe_2O_3 content in ferrosiliceous sacrificial concrete.

3.3. H_2O Content. During MCCI, the generated H_2O from concrete decomposition arises through the melt pool. On one hand, H_2O can react with the metal in the melt to release H_2. On the other hand, the gas bubble stirs the melt, which can facilitate to the heat transfer and the mixing of different layers. In this regard, the H_2O content is another important factor for MCCI. In this paper, the H_2O content is chosen at 2%, 4.4%, and 8% to investigate the related effect on MCCI. The other components are adjusted to maintain the sum of 100%. The enforced stratification is applied for the configuration of the pool.

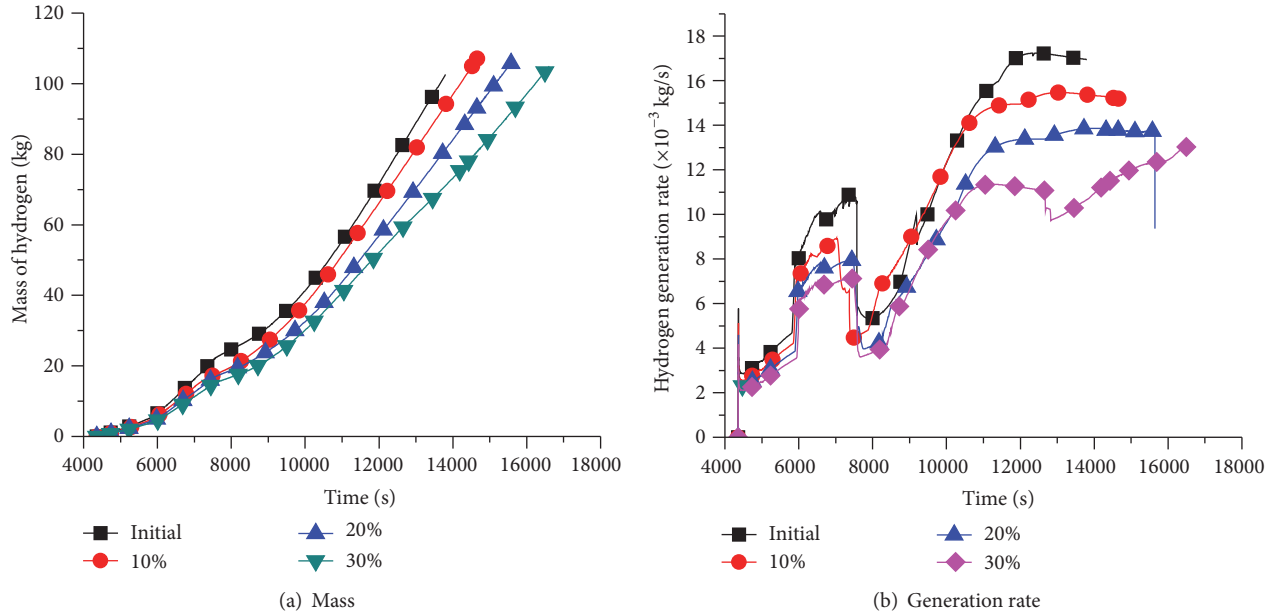

Figure 5: Hydrogen mass generation rate under different ablation enthalpy.

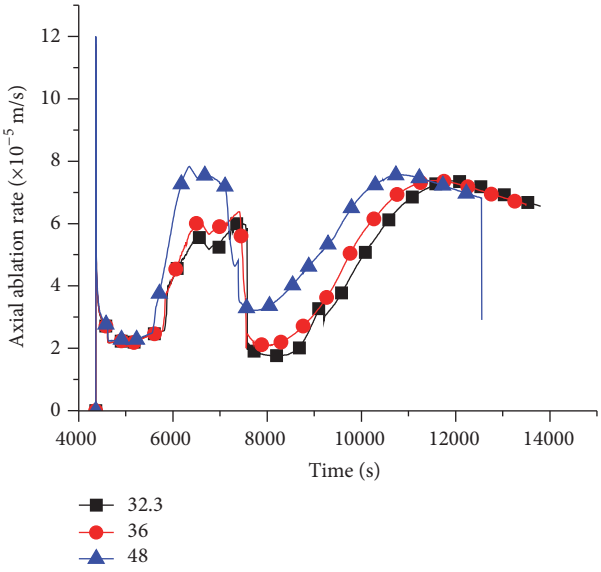

Figure 6: Sacrificial concrete ablation rate under different contents of Fe_2O_3.

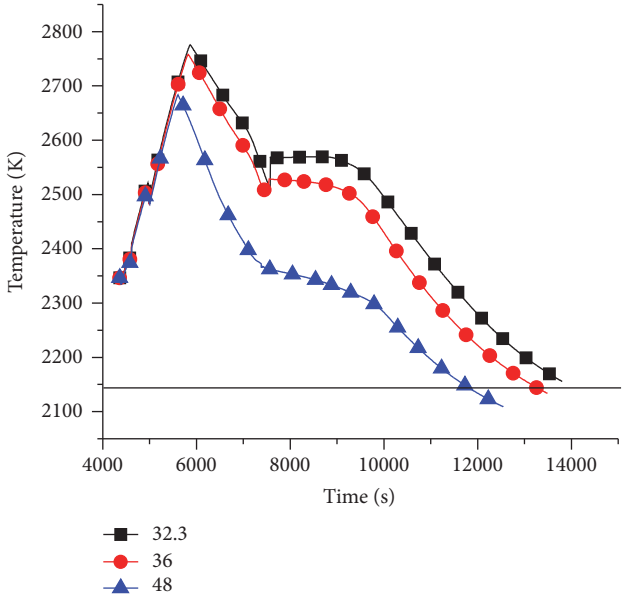

Figure 7: Temperature under different contents of Fe_2O_3.

As shown in Figure 11(a), with the increase of H_2O content, the ablation depth of sacrificial concrete decreases during most period of MCCI. It is noted that, at the elapsed time of 11698~14446 s, the sacrificial concrete ablation depth for the 4.4% H_2O content is larger than that for the 2% H_2O content. As shown in Figure 11(b), little difference can be detected for the sacrificial concrete ablation rate before 7730 s. After 7730 s, however, the ablation rate varies sharply after a period of slow ablation due to the appearance and disappearance of the LOX layer. For the sacrificial concrete with 2% H_2O, the ablation rate increases sharply in 11689~14288 s. It is caused by the sharp increase of heat transferred to sacrificial concrete due to the disappearance of the LOX layer above MET and HOX layers. Thereafter, the sacrificial concrete ablation rate decreases dramatically till 16138 s. The average ablation rate is around 2.80×10^{-5}~2.90×10^{-5} m/s with a peak value of 1.05×10^{-4} m/s till the basemat is melted through. The overall tendency of ablation rate of the 4.4% H_2O content is similar to that of the 2% H_2O content. Some variations occur 9500~15343 s. The maximum ablation rate reaches 7.5×10^{-5} m/s for the sacrificial concrete with 4.4% H_2O content, lower than that of concrete with 2% H_2O

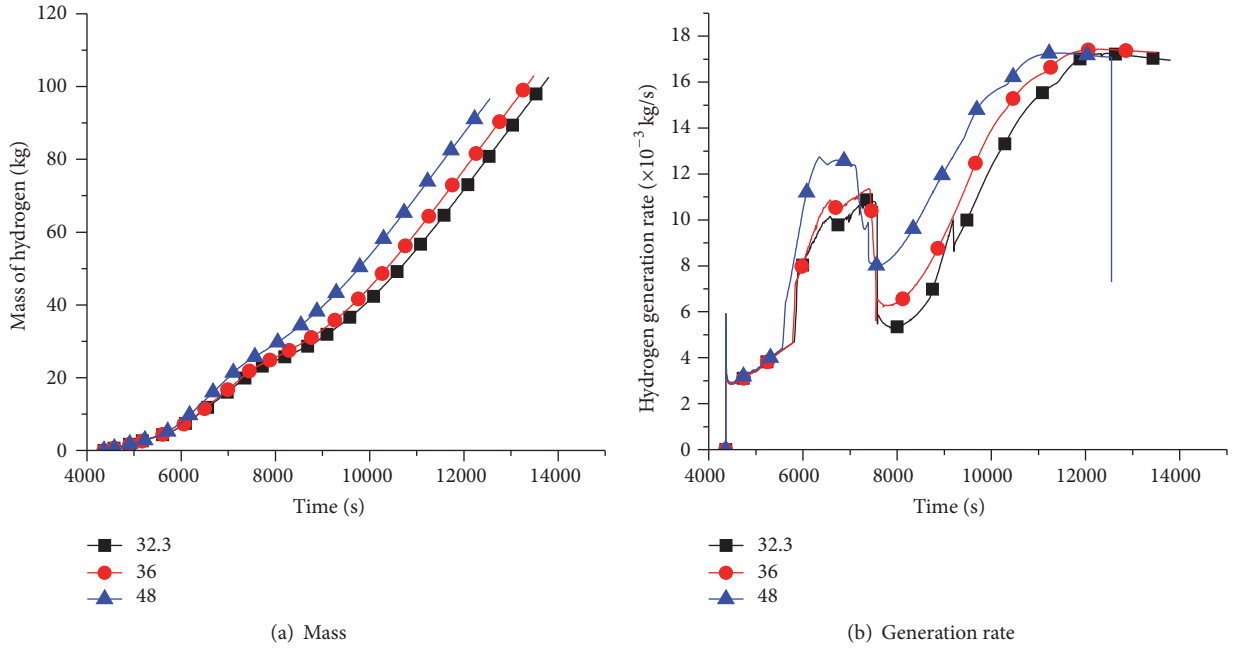

(a) Mass (b) Generation rate

Figure 8: Hydrogen mass generation rate under different contents of Fe_2O_3.

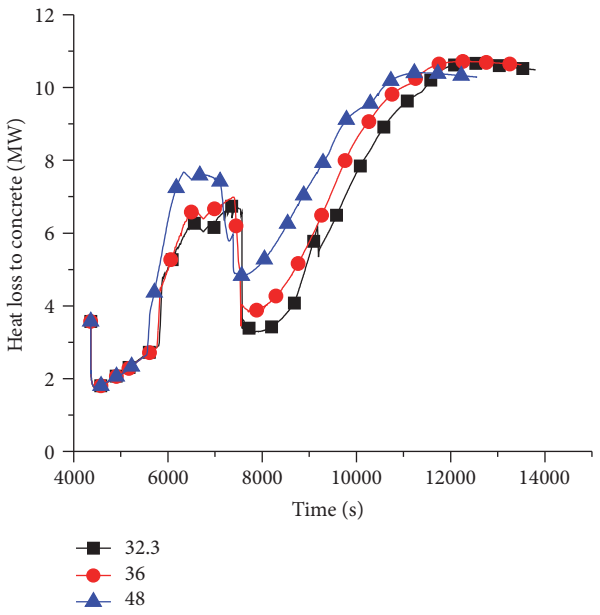

Figure 9: Heat loss to concrete under different contents of Fe_2O_3.

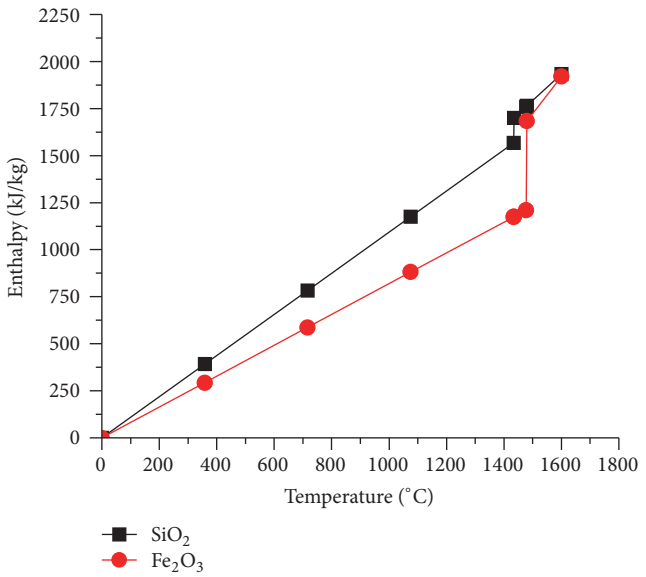

Figure 10: Enthalpy of quartz (SiO_2) and hematite (Fe_2O_3) [13].

content. After 15343 s, the ablation rate is 1.9~3.6 × 10^{-5} m/s and is also lower than that of concrete with 2% H_2O content. In addition, the ablation rate with 8% H_2O content is always at a low value of 1.33~1.70 × 10^{-5} m/s till 23480 s. It increases sharply till the sacrificial concrete is melted through due to the disappearance of the LOX layers after 23480 s. The melt-through time increases from 16005 s to 18130 s to 23622 s for the sacrificial concrete with 2%, 4.4%, and 8% H_2O content, respectively. Similar results were reported by Gencheva et al. [19]. On the whole, with the increase of H_2O content, the ablation rate of sacrificial concrete was decreased. Maybe that was because the bubbling caused by the higher H_2O content could result in mixing and thus lead to an even slower axial ablation rate [20].

In addition, the temperatures of HOX and MET decrease with the increase of H_2O content in sacrificial concrete, as illustrated in Figure 12.

As shown in Figure 13, the hydrogen mass and the generation rate of concrete with 8% H_2O content are both higher than those of concrete with 2% and 4.4% H_2O content, which differs from its ablation depth and rate. The total mass

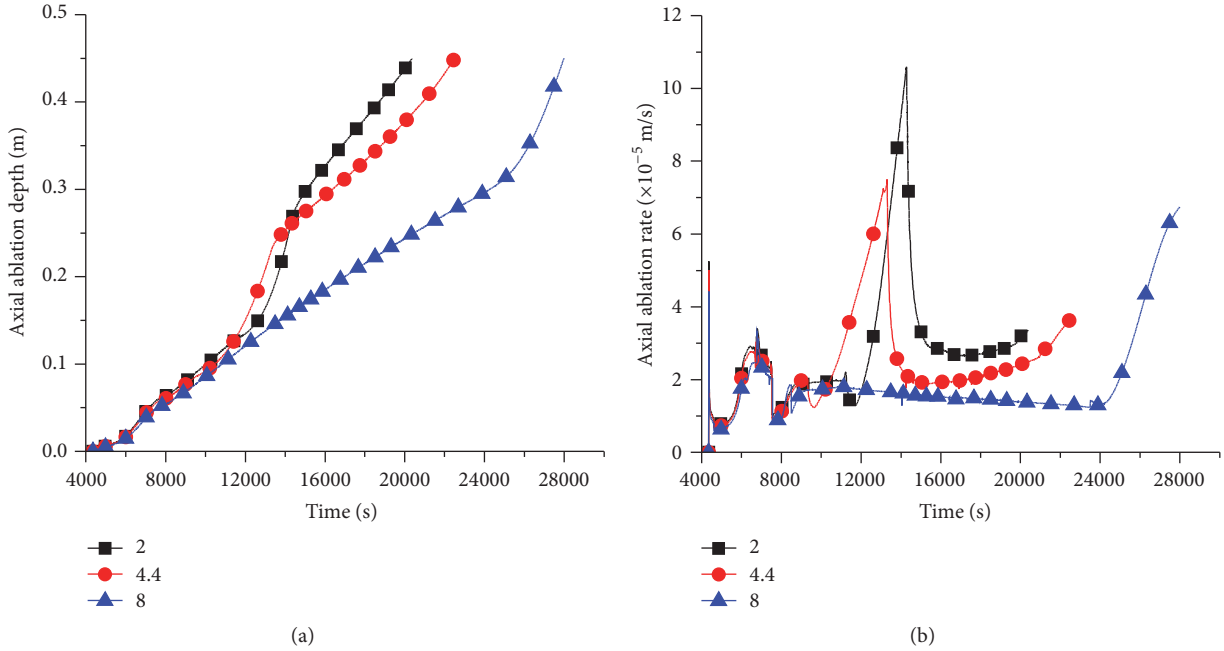

Figure 11: (a) Sacrificial concrete ablation depth and (b) ablation rate under different contents of H_2O as a function of time.

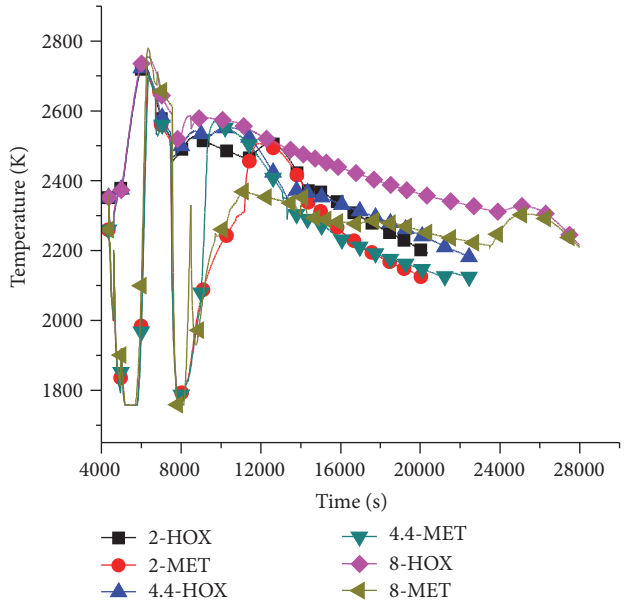

Figure 12: Temperature of HOX and MET under different contents of H_2O.

of hydrogen generated for the 8% H_2O content is 389.42 kg, and it is 3.6 times of that generated for the 2% H_2O content. Therefore, the higher H_2O content could lead to the increase of H_2 explosion possibility in reactor, which affects the safety of NPP.

As shown in Figure 14, the small thickness of LOX varies mildly with the H_2O content before 7300 s. As the sacrificial concrete ablates, the thickness of LOX for the sacrificial concrete with 2% H_2O content increases rapidly at 11698~144258 s. The related elapsed time is at 9500~13231 s for the sacrificial concrete with 4.4% H_2O content, while no LOX layer can be detected until 23480 s for the sacrificial concrete with 8% H_2O content. It might be attributed to the larger mass of heavy ZrO_2 generated by the Zr—H_2O reaction. The gas mass generated during MCCI increases with the increase of H_2O content, which results in more heat loss to surface and less heat loss to sacrificial concrete, as can be seen in Figures 15 and 16. Most of all, for the sacrificial concrete with 8% H_2O content, the heat loss to surface by generated gas is about 10 times of that to sacrificial concrete ablation. In this regard, the ablation rate decreases with the decrease of H_2O content. In addition, the LOX MET and HOX hinder heat loss through the surface of melt, as illustrated in Figure 16. The ablation rate increases sharply when the LOX exists. Consequently, the H_2O content has a big effect on the ablation rate and hydrogen production of MCCI, and the H_2O content of sacrificial concrete is the lower the better for the safety of nuclear power plant.

In a word, the properties of sacrificial concrete have a crucial impact on the MCCI. In practice, the ablation enthalpy of sacrificial concrete is the higher the better, while the H_2O and Fe_2O_3 content of sacrificial concrete is the lower the better for the safety of NPP and for the nuclear accident mitigation. The simulation investigation has important consulting meaning to the mixture design of the ferrosiliceous sacrificial concrete.

4. Conclusion

In this paper, based on the computer code MELCOR, we investigate the effects of sacrificial concrete properties on MCCI, including its ablation enthalpy and contents of Fe_2O_3 and H_2O. In particular, the ferrosiliceous concrete used in

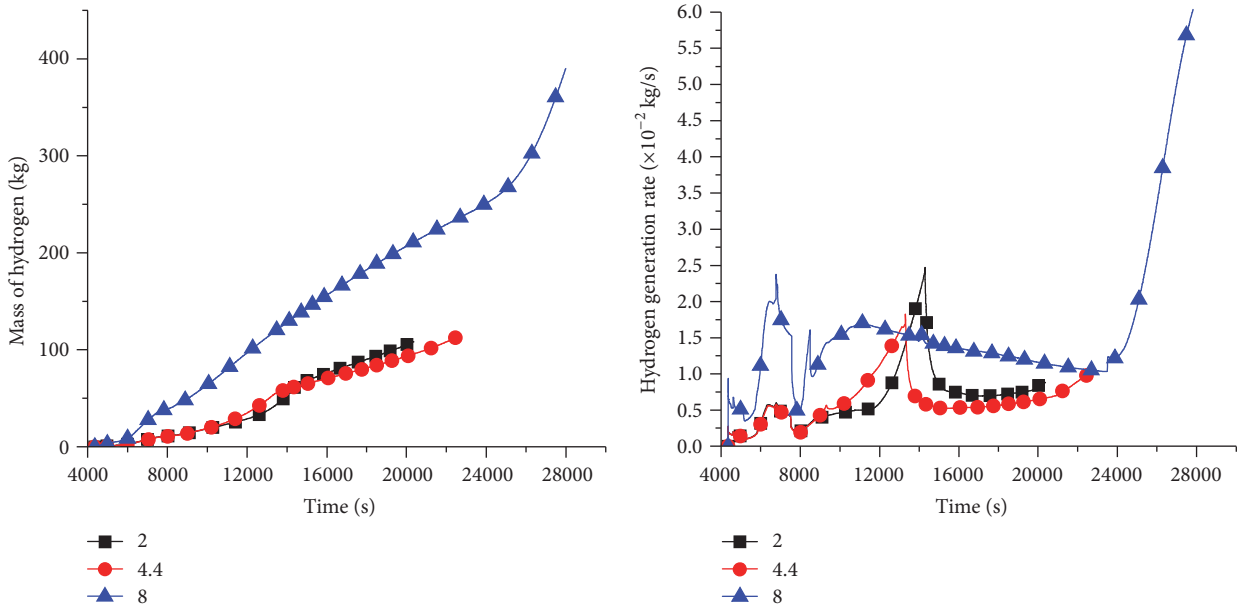

(a) Mass (b) Hydrogen generation rate

Figure 13: Hydrogen mass and generation rate under different contents of H_2O.

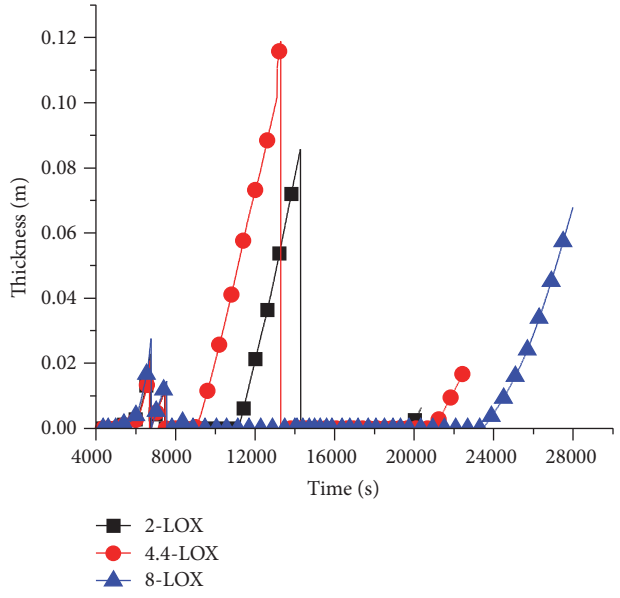

Figure 14: Thickness of LOX under different contents of H_2O.

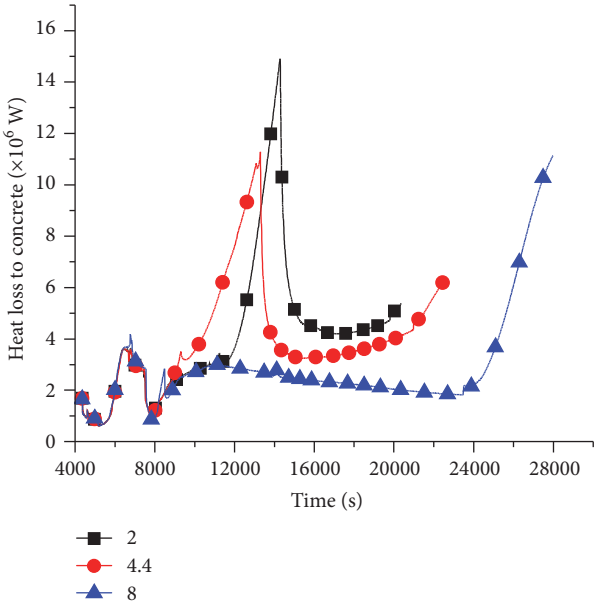

Figure 15: Heat loss to sacrificial concrete under different contents of H_2O.

EPR is examined upon a typical small break loss of coolant severe accident. Relevant parameters are discussed, including the sacrificial concrete ablation rate, the temperature of the melt, and the mass and generation rate of hydrogen. Some general conclusions can be drawn as follows:

(1) As the sacrificial concrete ablation enthalpy increases, its ablation rate decreases, and meanwhile the melt-through time of basemat increases. With the higher sacrificial concrete ablation enthalpy, the hydrogen generation rate is lower, and the temperature decreases faster. Besides that, little difference can be detected in the total hydrogen mass.

(2) The higher Fe_2O_3 content leads to the larger ablation rate as well as hydrogen generation rate, but little difference exists for the total masses of hydrogen. A faster decrease of temperature is detected at the melt pool.

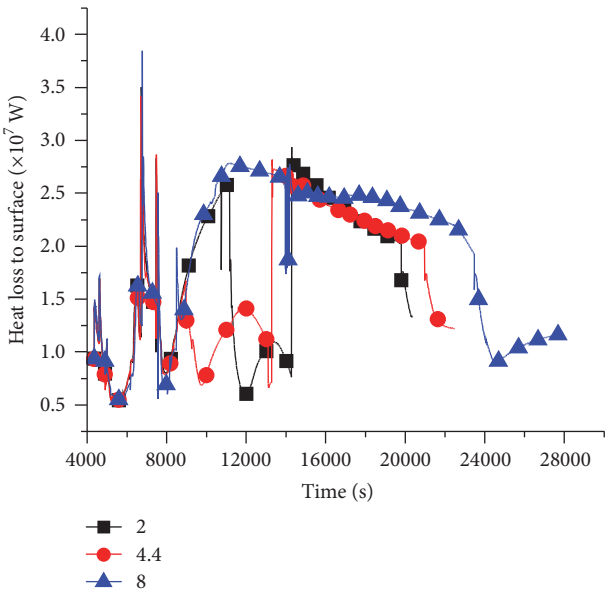

FIGURE 16: Heat loss to surface under different contents of H_2O.

(3) When LOX appears in the melt, the sacrificial concrete ablation rate increases rapidly. The quick decrease of heat to the surface results in the sharp increase of heat transmitted to sacrificial concrete. Most of all, the ablation rate of sacrificial concrete decreases with the increased H_2O content. Compared with the 2% H_2O content, the melt-through time and total hydrogen mass for the 8% H_2O content are 0.48 and 2.6 times larger, respectively.

(4) In practice, the ablation enthalpy of sacrificial concrete is the higher the better, while the Fe_2O_3 and H_2O content of sacrificial concrete is the lower the better.

(5) The simulation study has significant consulting meaning to the mix proportion design of the ferrosiliceous sacrificial concrete.

Competing Interests

The authors declare that there is no conflict of interests regarding the publication of this paper.

Acknowledgments

The investigation is finically supported by China National Natural Science Funding Committee (nos. 51378114 and 5161113020), National Basic Research Program of China (973 program, 2015CB655105), and Transformation of Major Scientific and Technological Achievements of Jiangsu Province Funded Projects (no. 85120000220), which are gratefully appreciated.

References

[1] T. Sevón, T. Kinnunen, J. Virta, S. Holmström, T. Kekki, and I. Lindholm, "HECLA experiments on interaction between metallic melt and hematite-containing concrete," *Nuclear Engineering and Design*, vol. 240, no. 10, pp. 3586–3593, 2010.

[2] T. Sevón, C. Journeau, and L. Ferry, "VULCANO VB-U7 experiment on interaction between oxidic corium and hematite-containing concrete," *Annals of Nuclear Energy*, vol. 59, no. 9, pp. 224–229, 2013.

[3] B. Eppinger, F. Fellmoser, G. Fieg, H. Massier, and G. Stern, "Experiments on concrete erosion by a corium melt in the EPR reactor cavity: KAPOOL 6-8," Forschungszentrum Karlsruhe Technik und Umwelt Wissenschaftliche Berichte FZKA 6453, 2000.

[4] W. Widmann, M. Bürger, G. Lohnert, H. Alsmeyer, and W. Tromm, "Experimental and theoretical investigations on the COMET concept for ex-vessel core melt retention," *Nuclear Engineering and Design*, vol. 236, no. 19–21, pp. 2304–2327, 2006.

[5] M. T. Farmer, S. Lomperski, D. J. Kilsdonk, R. W. Aeschlimann, and S. Basu, "OECD MCCI project 2-D core concrete interaction (CCI) tests: CCI-3 test data report-thermal hydraulic results. Rev. 0 October 15, 2005," *Transactions of the Royal Entomological Society of London*, vol. 11, no. 1, pp. 715–721, 2005.

[6] C. Journeau, P. Piluso, J.-F. Haquet et al., "Two-dimensional interaction of oxidic corium with concretes: The VULCANO VB test series," *Annals of Nuclear Energy*, vol. 36, no. 10, pp. 1597–1613, 2009.

[7] M. Fischer, "The severe accident mitigation concept and the design measures for core melt retention of the European Pressurized Reactor," *Nuclear Engineering and Design*, vol. 230, no. 1–3, pp. 169–180, 2004.

[8] H.-Y. Chu, J.-Y. Jiang, W. Sun, and M. Zhang, "Thermal behavior of siliceous and ferro-siliceous sacrificial concrete subjected to elevated temperatures," *Materials and Design*, vol. 95, pp. 470–480, 2016.

[9] H. Chu, J. Jiang, W. Sun, and M. Zhang, "Mechanical and physicochemical properties of ferro-siliceous concrete subjected to elevated temperatures," *Construction and Building Materials*, vol. 122, pp. 743–752, 2016.

[10] J. Wang, Y. Zhang, K. Mao et al., "MELCOR simulation of core thermal response during a station blackout initiated severe accident in China pressurized reactor (CPR1000)," *Progress in Nuclear Energy*, vol. 81, pp. 6–15, 2015.

[11] M. Nie, *Temporary Melt Retention in the Reactor Pit of the European Pressurized Water Reactor (EPR)*, 2005.

[12] R. O. Gaunt, R. K. Cole, C. M. Erickson et al., *MELCOR Computer Code Manuals: Primer and Users' Guides Version 1.8.5*, NUREG/CR-6119, SAND2000-2417/1, vol. 1, 1994.

[13] T. Sevon, *Molten Core-Concrete Interactions in Nuclear Accidents: Theory and Design of an Experimental Facility*, 2005.

[14] D. R. Bradley, D. R. Gardner, J. E. Brockmann, and R. O. Griffith, *Corcon-mod3: An Integrated Computer Model for Analysis of Molten Core-concrete Interactions. User's Manual*, Nuclear Fuel Cycle and Fuel Materials, 1993.

[15] G. A. Greene, "Heat, mass, and momentum transfer in a multifluid bubbling pool," *Advances in Heat Transfer*, vol. 21, pp. 277–346, 1991.

[16] S. S. Kutateladze and I. G. Malenkov, "Boiling and bubbling heat transfer between a gas-liquid system and a heat exchange element," *Journal of Applied Chemistry of the USSR*, vol. 35, no. 11, 1962.

[17] L. Tong, X. Cao, J. Li, and Y. Yang, "Model comparisons on molten core-concrete interactions," *Nuclear Science and Techniques*, vol. 20, pp. 251–256, 2009.

[18] M. Nie, "Sacrificial concrete layer thickness in the core catcher," Tech. Rep., Revision A, Framatome ANP, 2004.

[19] R. Gencheva, A. Stefanova, and P. Groudev, "ASTECv2/MEDICIS computer code investigation of influence of water content and carbon dioxide content in the concrete on the kinetics of molten corium-concrete interaction," *Nuclear Engineering and Design*, vol. 265, pp. 625–632, 2013.

[20] P. Dejardin and L. Sallus, "Parametrical study on MCCI reactor cases under dry cavity conditions for assessment of parameters of importance," in *Proceedings of the 5th European Review Meeting on Severe Accident Research (ERMSAR '12)*, Cologne, Germany, March 2012.